Soliton dynamics of nonlinear diatomic lattices

St. Pnevmatikos*
Laboratoire d'Optique du Réseau Cristallin, 6 boulevard Gabriel, Université de Dijon, 21100 Dijon, France

N. Flytzanis
Department of Physics, University of Crete and Research Center of Crete, 71110 Heraklio, Crete, Greece

M. Remoissenet
Laboratoire d'Optique du Réseau Cristallin, 6 boulevard Gabriel, Université de Dijon, 21100 Dijon, France
(Received 22 March 1985)

We study analytically and numerically a nonlinear diatomic chain with cubic and/or quartic interaction potential between first- and second-nearest neighbors. In the continuum approximation using a decoupling *ansatz* for the motion of the two different sublattices we obtain supersonic or subsonic acoustic kink (pulse) solitons, long-wavelength acoustic oscillating solutions of breather type, and purely optical-envelope-type excitations. We then introduce an analytical technique which enables us to calculate oscillating soliton solutions of the symmetric or asymmetric envelope or hole (dark) type, modulating a quasiharmonic carrier the wave vector of which is not limited to long wavelength. The characteristic energies of all these kinds of excitations are given as a function of the main parameter. Numerical simulations on their propagation and interactions show these excitations to be long-lived quasisolitons.

I. INTRODUCTION

The study of the dynamics of nonlinear lattices and the related solitonlike excitations has been greatly influenced by the pioneering works of Fermi, Pasta, and Ulam[1] and of Zabusky and Kruskal.[2] Most of the work in this area has considered acoustic "in phase" modes in models of one-dimensional (1D) monoatomic chains,[3,4] the prototype of which is the Toda lattice[5] with exponential atomic interactions. In comparison, the dynamics of nonlinear excitations in diatomic chains has received much less attention and only recently, due to the analytical complexities involved. Models of diatomic lattices have been used as prototypes to approach the transport of energy,[6] the dynamics of real materials (like ferroelectric perovskites), which present a quasi-1D diatomic structure along certain crystallographic directions.[7,8] For complicated polyatomic systems like molecular-hydrogen-bonded chains,[9] polymers,[10] or biomolecules[11] the problem becomes tractable by selecting the most important degrees of freedom and using a diatomic model.

Zabusky and Deem[12] were the first to show by numerical simulations that nonlinear optical excitations ("out of phase" modes) created with arbitrary optical Gaussian initial conditions can propagate in a monoatomic anharmonic chain with cubic interatomic interactions. Based on the Korteweg–de Vries (KdV) equation, Tasi and Musgrave[13] and Tasi[14] made an analysis of the far-field response of a diatomic chain to a shock-type acoustic initial excitation. Büttner and Bilz[15] have proposed a model of a diatomic chain with quartic nonlinear interactions. Using an appropriate decoupling technique in the continuum limit they have shown that acoustic and optical kinklike excitations exist (the optical kink is for a displasive-type interaction) which are, respectively, solutions of a KdV and ϕ^4 equations. Furthermore, it was independently shown that when the interatomic potential has a cubic nonlinearity, the dynamics of the diatomic chain may support, in the continuum limit, optical-envelope modes coupled with acoustic modes,[16,17] which are decoupled for a quartic nonlinearity.[18] The coupling between diatomic chains was examined[19] in order to model certain ferroelectric materials. All the preceding results are analytical in the continuum limit and for models where the coupling between atoms is limited to first-neighbor interactions (FNI).

In this paper we present the important and new features which emerge from a systematic analytical and numerical study of the dynamics of the nonlinear and nontopological excitations of a diatomic chain model. In Sec. II we present the model with a nonlinear quartic and cubic coupling potential which includes second-neighbor interactions (SNI). In Sec. III we use the continuum approximation and apply a decoupling ansatz to obtain the kink solitons (Secs. III A–III C) or the long-wavelength oscillatory excitations of breather type (Sec. III D) or purely optical-envelope type (Sec. III E). Simultaneously we discuss their properties. In Sec. IV we describe the method (semidiscrete approximation) to obtain the short-wavelength envelope solitons and present the results for the behavior of the solutions in computer simulations. In Sec. V we present a model of two parallel interacting chains which is related to the previous diatomic model chain. In the final section we present concluding remarks and possible extensions of the present model.

II. THE MODEL

We consider a chain in one dimension with two atoms of masses M_1 and M_2 per unit cell with a spacing of $2D$

between cells (see Fig. 1). The atoms move longitudinally interacting with their first (FNI) and second nearest neighbors (SNI). The interaction potential between atoms is a polynomial approximation to realistic potentials and has the form

$$V_i(r_{ln})=\tfrac{1}{2}G_i r_{ln}^2+\tfrac{1}{3}A_i r_{ln}^3+\tfrac{1}{4}B_i r_{ln}^4 , \tag{2.1}$$

where r_{ln} is the relative displacement between the lth and nth atoms from equilibrium (the indices n and l indicate the atom number and not the cell). The index i takes the values 0, 1, or 2 depending whether (2.1) describes FNI, or SNI between masses M_1, or SNI between masses M_2, respectively. In the following we shall neglect the index i when $i=0$ so that the corresponding force constants are G, A, and B. Longer-range interactions[20] are neglected here.

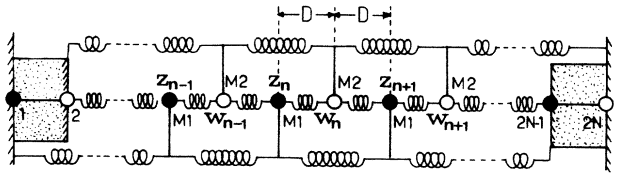

FIG. 1. Diatomic chain model with FNI and SNI.

If we denote by z_n (w_n) the displacement from equilibrium of the atom with mass M_1 (M_2) correspondingly in the nth cell the equations of motion can be written as

$$M_1\ddot{z}_n = G(w_n-2z_n+w_{n-1})+G_1(z_{n+1}-2z_n-z_{n-1})+A[(w_n-z_n)^2-(z_n-w_{n-1})^2]+A_1[(z_{n+1}-z_n)^2-(z_n-z_{n-1})^2]$$
$$+B[(w_n-z_n)^3-(z_n-w_{n-1})^3]+B_1[(z_{n+1}-z_n)^3-(z_n-z_{n-1})^3] , \tag{2.2a}$$
$$M_2\ddot{w}_n = G(z_{n+1}-2w_n+z_n)+G_2(w_{n+1}-2w_n-w_{n-1})+A[(z_{n+1}-w_n)^2-(w_n-z_n)^2]+A_2[(w_{n+1}-w_n)^2-(w_n-w_{n-1})^2]$$
$$+B[(z_{n+1}-w_n)^3-(w_n-z_n)^3]+B_2[(w_{n+1}-w_n)^3-(w_n-w_{n-1})^3] , \tag{2.2b}$$

where the overdot $(\cdot)$ denotes time differentiation, and $n=1,2\ldots,N$, where N is the number of cells considered.

In (2.2) we have $2N$ coupled nonlinear difference-differential equations for z_n and w_n. However, to be able to apply the analytical techniques that were used in monoatomic chains,[21,22] we must find some method to decouple the two functions $z_n(t)$ and $w_n(t)$, as will be described in Sec. III, when we go to the continuum approximation. In (2.2) we have not included any phenomenological damping mechanisms, except due to discretization effects which will be presented elsewhere.[23] They could be important for narrow solitons. Here we must point out that due to the discreteness of the chain, the solutions for the diatomic chain are quasisolitons in the sense that there is some energy loss during propagation or collision which is very small for wide solitons. Also, we will not consider the effect of an external driving force. Details of the numerical simulations with initial conditions the solitons obtained in Secs. III–V, are described elsewhere.[24]

III. SOLITONS IN THE CONTINUUM APPROXIMATION

A. The decoupling ansatz

For a nonlinear monoatomic chain the large width kink solitons can be described by a single smooth curve since the displacement $y_n(t)$ varies slowly. For optical-type oscillations in a linear diatomic chain the ratio of the displacements of two neighboring atoms is inversely proportional to the ratio of their masses and the two atoms move out of phase. Thus we expect that for a nonlinear diatomic chain we need two smooth functions $z_n(t)$ and $w_n(t)$ for the displacement of the odd (M_1) and even (M_2) masses. We apply the continuum approximation for the displacement of each mass separately, i.e., if we let $x=2nD$ we have

$$z_{n\pm1}=z\pm2Dz_x+2D^2z_{xx}\pm\tfrac{4}{3}D^3z_{xxx}+\tfrac{2}{3}D^4z_{xxxx}+\cdots , \tag{3.1}$$

with a similar expression for $w_{n\pm1}$. By using expression (3.1), we transform the system of difference-differential equations (2.2) into two partial differential equations for $z(x,t)$ and $w(x,t)$ which are coupled. The solution of the system is simple if we can relate the two displacements, in analogy with the linear diatomic chain.

To decouple the two equations we use the following ansatz[15] by expanding $w(x,t)$ in terms of the displacement $z(x,t)$ and its derivatives

$$w(x,t)=\sigma\left[z+b_1Dz_x+\frac{b_2}{2}D^2z_{xx}+\frac{b_3}{3}D^3z_{xxx}+\frac{b_4}{24}D^4z_{xxxx}+b_0f(z,z_x,\ldots)\right]+O(\epsilon^{4+r}) , \tag{3.2}$$

where ϵ is a small parameter that scales changes in the displacements with $r=1$ or 2 depending on the potential of interaction.[21] The procedure is to substitute $w(x,t)$ from (3.2) and its derivatives in the continuum approximation of the equation of motion (2.2) and impose that

the two equations in (2.2) for $z(x,t)$ are equivalent. This will determine the possible values for the parameter σ and the corresponding ones for b_1, b_2, b_3, b_4, and b_0. In the continuum approximation there are two values for $\sigma=1$ or $-M_1/M_2$. In analogy with the linear chain the $\sigma=1$ solution corresponds to an acoustic mode where the atoms move in phase with slowly varying amplitudes. The value $\sigma=-M_1/M_2$ gives a nonlinear optical mode where the atoms move out of phase with amplitude ratios equal to σ. The solution of one of the identical equations will give the displacement of the odd atoms $z(x,t)$, while $w(x,t)$ for the even atoms can be obtained from the ansatz (3.2). In what follows we shall present the solutions for the different modes. The last term $f(z,z_x,\dots)$ in the expansion (3.2) is a nonlinear function of z and its derivatives. For simple potentials (i.e., quartic) b_0 turns out to be zero if we keep low-order terms in ϵ and no SNI. For a more general potential we need $b_0\neq 0$, and the form of $f(z,z_x,\dots)$ can be guessed. In the expansion of (3.2) we can also include time derivatives of z.

B. Acoustic mode ($\sigma=1$)

In writing expansions (3.1) and (3.2) we have scaled the space and time derivatives as $\partial/\partial x\sim O(\epsilon)$ and $\partial/\partial t\sim O(\epsilon)$, and we have neglected consistently high order in ϵ terms. Therefore, we keep up to fourth derivatives of z or w and the appropriate nonlinear terms (different for the cubic and the quartic potential) to balance dispersion and nonlinearity. By following the procedure described earlier we can obtain the coefficients in (3.2) for the acoustic mode ($\sigma=1$) and obtain

$$b_1=1,\quad b_2=2\mu_0\left[\frac{1}{M_2}-2g_0\right],$$
$$b_3=6\mu_0\left[\frac{2M_1-M_2}{3M_1M_2}-2g_0\right], \tag{3.3}$$
$$b_4=24\mu_0\left[\frac{1}{3M_2}-\frac{b_2^2}{4M_1}-2g_0\left[\frac{b_2}{2}+\frac{1}{3}\right]\right],$$

with

$$\mu_0=\frac{M_1M_2}{M_1+M_2} \tag{3.4}$$

and

$$g_1=\frac{G_1}{G},\quad g_2=\frac{G_2}{G},\quad g_0=\frac{g_1}{M_1}-\frac{g_2}{M_2}. \tag{3.5}$$

If we include second-neighbor interactions, i.e., $g_1,g_2\neq 0$, to satisfy the compatibility conditions between the two equations for z and w, we must use the nonlinear term in expansion (2.3) which, for the case of the quartic potential, is chosen as

$$b_0f(z,z_x,\dots)=b_0D^4z_x^2z_{xx}, \tag{3.6}$$

with

$$b_0=\frac{3\mu_0}{G}\left[2Bg_0-8\left[\frac{B_1}{M_1}-\frac{B_2}{M_2}\right]\right]. \tag{3.7}$$

The effect of this term is an infinitesimal change in $w(x,t)$ from (3.2) since it is of $O(\epsilon^4)$ [if $z\sim O(1)$]. On the other hand it can change the coefficients of the nonlinear terms of the resulting continuum equation for $z(x,t)$, thus modifying the properties of z (and consequently of w) such as the width, amplitude, etc.

After evaluation of the coefficients b_i ($i=0,\dots,4$) from the compatibility condition, we obtain a single equation in the form of a generalized Boussinesq (G-Bq) equation for $u=z_x$ as

$$u_{tt}=c_0^2u_{xx}+\frac{p_0}{2}(u^2)_{xx}+\frac{q_0}{3}(u^3)_{xx}+h_0u_{xxxx}, \tag{3.8}$$

with

$$c_0^2=\frac{2G}{M_1}\left[\frac{b_2}{2}+2g_1\right]D^2$$
$$=\frac{2G}{M_1+M_2}D^2[1+2(g_1+g_2)], \tag{3.9a}$$
$$p_0=\frac{4}{M_1}\left[A\frac{b_2}{2}+4A_1\right]D^3, \tag{3.9b}$$
$$q_0=\frac{6}{M_1}\left[B\frac{b_2}{2}+8B_1+\frac{b_0}{3}\right]D^4, \tag{3.9c}$$
$$h_0=\frac{2G}{M_1}\left[\frac{b_4}{24}-\frac{b_3}{6}+\frac{b_2}{2}-\frac{1}{3}+\frac{2}{3}g_1\right]D^4, \tag{3.9d}$$

where the speed of sound c_0, the dispersion parameter h_0, and the nonlinear coefficients p_0 and q_0 depend on the interaction potential. The linear part of (3.8) for $h_0>0$ describes the propagation of plane waves with a dispersion relation $\omega^2(k)=c_0^2k^2-h_0k^4$, which implies an instability for $k^2>c_0^2/h_0$. One could say that it is not possible to construct a stable wave packet from the normal modes of the linear system since short-wavelength components would rapidly diverge. This is not troublesome however, since Eq. (3.12) describes only long-wavelength propagation outside the range of instability. In fact, no simulations on the propagation of solitary waves have shown such an instability for the discrete lattice as predicted in an elaborate analysis.[25] If in (3.8), with the coefficients given by (3.9), we neglect the cubic part of the interaction potential and limit ourselves to velocities near the speed of sound, we obtain a modified KdV (M-KdV) equation and reproduce[24] the results of Ref. 15. For the limit $M_1=M_2$, the results for the monoatomic chain are obtained[21,22,26] and (3.2) is a Taylor expansion of the even atom displacements around the odd ones.

The kink-type solutions for (3.8) are presented in Ref. 21 for the monoatomic chain and here we give the analytical expression for the general case ($p_0\neq 0$, $q_0\neq 0$) as

$$z=\pm 2\,\mathrm{sgn}(h_0)\left[\frac{6h_0}{q_0}\right]^{1/2}\tan^{-1}\left[\frac{1}{W}\tanh\left[\frac{x-vt}{L}+x_1\right]\right], \tag{3.10}$$

with

$$W=\left[\frac{[p_0^2+6(v^2-c_0^2)q_0]^{1/2}\pm p_0}{[p_0^2+6(v^2-c_0^2)q_0]^{1/2}\mp p_0}\right]^{1/2} \tag{3.11}$$

and

$$L=2\left[\frac{h_0}{v^2-c_0^2}\right]^{1/2}. \tag{3.12}$$

In (3.10), x_1 is an arbitrary constant that defines the initial position of the soliton while v is the velocity. The signs (+) or (−) in (3.10) denote that the solution can be either dilatational or compressional. The parameter $\mathrm{sgn}(h_0)=\pm 1$ depending on the sign of h_0.

The width of the soliton depends on both the parameters W and L except when either $p_0=0$ or $q_0=0$, where only L is important. The parameter L must be multiplied by a numerical factor to give us the halfwidth at half height. The special cases $p_0=0$ or $q_0=0$ reduce to the Boussinesq (Bq) or modified Boussinesq (M-Bq) solitons.[24] The possible types of solutions (compressive or dilatational) are summarized in Table I, depending on the signs of h_0, p_0, and q_0. In (3.10) and (3.12) the quantities h_0/q_0 and $h_0/(v^2-c_0^2)$ must be positive. Table I is subject to the restriction that the values of h_0, p_0, q_0, and the soliton velocity are such that the continuum approximation is obeyed, and there are no discretization effects.[23] An acoustic-type soliton presents a net dilation related to the soliton mass which is a constant of the motion to $O(\epsilon)$. For the quartic potential it is independent of the velocity (true only in the continuum approximation) and depends only on the potential parameters. For a purely cubic potential, however, the amplitude (A_m) and, consequently, the mass depends on the velocity like $(v^2-c_0^2)^{1/2}$ for the Bq solution and $(v-c_0)^{1/2}$ for the KdV solution.[21,22] For the full potential (cubic and quartic), near the speed of sound, there are two different solutions one of which behaves like the cubic potential solution with amplitude proportional to $(v^2-c_0^2)^{1/2}$ and another one with a large amplitude but velocity independent. This can be seen by taking the appropriate limits in (3.10) and (3.11). The large-amplitude solution is denoted by an asterisk in Table I and could be unstable due to discretization effects.[24]

Solution (3.10) is valid near c_0. To study the properties of solitons with velocity away from c_0 we performed computer simulations (using 3.10) as initial conditions for propagation in a discrete lattice. The initial kink within a very short propagation time adjusts to a wave form with a new shape. In Fig. 2 we plot in (a) the variation of the width parameter L and in (b) the amplitude A_m of the particle displacement as a function of the normalized velocity v/c_0 of the kink. We see that when the width (L) is less than 3, the soliton relaxes in a new form but it preserves the portion of energy devoted to potential or kinetic the same as for the Bq. Once these solutions adjust to the discrete lattice they behave like solitons. For velocities near the speed of sound (within 5%) the agreement of (3.10) with the numerical solution is very good. For the M-Bq or G-Bq cases we have similar curves.

In Fig. 3 we plot the total energy of the kink soliton on a diatomic chain with a cubic [Fig. 3(a)] or a quartic potential [Fig. 3(b)] as a function of the normalized kink velocity v/c_0 for different mass ratios. For supersonic velocities ($v/c_0>1$), in the region where the continuum approximation is valid, the energy increases when the ratio M_2/M_1 strays from unity. Near $v/c_0=1$ the total energy behaves as follows: $[(v/c_0)^2-1]^{1/2}$ for the quartic potential and $[(v/c_0)^2-1]^{3/2}$ for the cubic potential. Therefore, the energy of the soliton in a quartic potential

TABLE I. Possible types of solutions for Eq. (3.8).

	Potential parameters		Kink soliton	Excitation produced on the lattice	Velocity
$h_0>0$	$p=0$	$q=0$	NO		
		$q>0$	YES	rarefaction or compression	
		$q<0$	NO		
	$p>0$	$q=0$	YES	rarefaction	Supersonic $v>c_0$
		$q>0$	YES	rarefaction or compression*	
		$q<0$	NO		
	$p<0$	$q=0$	YES	compression	
		$q>0$	YES	rarefaction* or compression	
		$q<0$	NO		
$h_0<0$	$p=0$	$q=0$	NO		
		$q>0$	NO		
		$q<0$	YES	rarefaction or compression	
	$p>0$	$q=0$	YES	compression	
		$q>0$	NO		Subsonic $v<c_0$
		$q<0$	YES	rarefaction* or compression	
	$p<0$	$q=0$	YES	rarefaction	
		$q>0$	NO		
		$q<0$	YES	rarefaction or compression*	

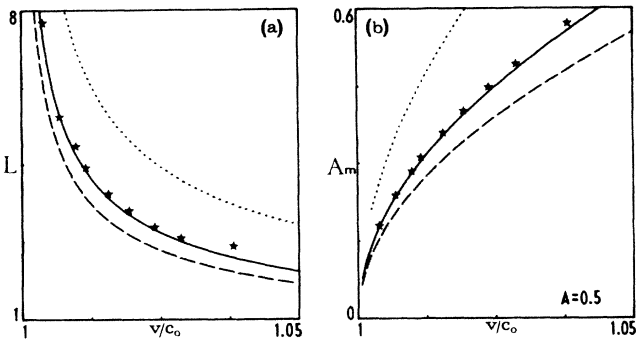

FIG. 2. Variation of (a) the width parameter L and (b) the amplitude A_m versus normalized soliton velocity v/c_0 for various mass ratios of the Bq soliton with $A=0.5$, $B=0$. Dashed, solid and dotted lines correspond to mass ratios $M_2/M_1=1$, 2, and 10, respectively. The stars are the results from numerical simulation after 100 time units of propagation on the discrete chain for the case $M_2/M_1=2$.

is larger for v near c_0, but is soon overcome by the cubic potential. The stars represent the results of a numerical simulation using Bq solitons as initial conditions and measuring their final total energy and velocity after propagation of 100 time units. The agreement with the theoretical curve is very good, so that the adjustment of the solitons in the lattice for this range of velocities is small. It should also be pointed out that the total energy is divided between potential and kinetic energy (dotted lines in Fig. 3) in such a way that the kinetic energy is slightly higher for supersonic solitons, while the opposite is observed for subsonic solitons.

In Fig. 4 we present the time evolution of the head-on collision of two solitons with velocities (widths) equal to $v_1=0.823$ ($L_1=5.272$) and $v_2=-0.822$ ($L_2=5.732$) in a diatomic chain with $M_1/M_2=2$ with FNI only, and a cubic interaction potential ($G=1, A=0.5, B=0$). In the plot we present the relative displacement between neighboring atoms which is related to $u(=z_x)$ at different propagation times and the collision is quasielastic with infinitesimal changes in the soliton forms.

Detailed computer simulations for various values of the parameters of the interaction potential including cubic and quartic terms show that the solutions of the continuum equations for large width are also good solutions for the discrete medium. Their propagation creates no radiation and their collisions are quasielastic. In general, there is a phase shift during collision of the order of a few lattice spacings. It can become significant however, for certain values of the parameter $h_0<0$, where the solitons behave quite different (resonance phenomena[27]). When the simulations are performed on a finite chain there is also a small phase shift due to scattering from a fixed boundary.

D. Breather solitons

For a quartic potential ($p_0=0$) in the continuum approximation and for velocities near the speed of sound, Eq. (3.8) reduces to the M-KdV equation, which also has

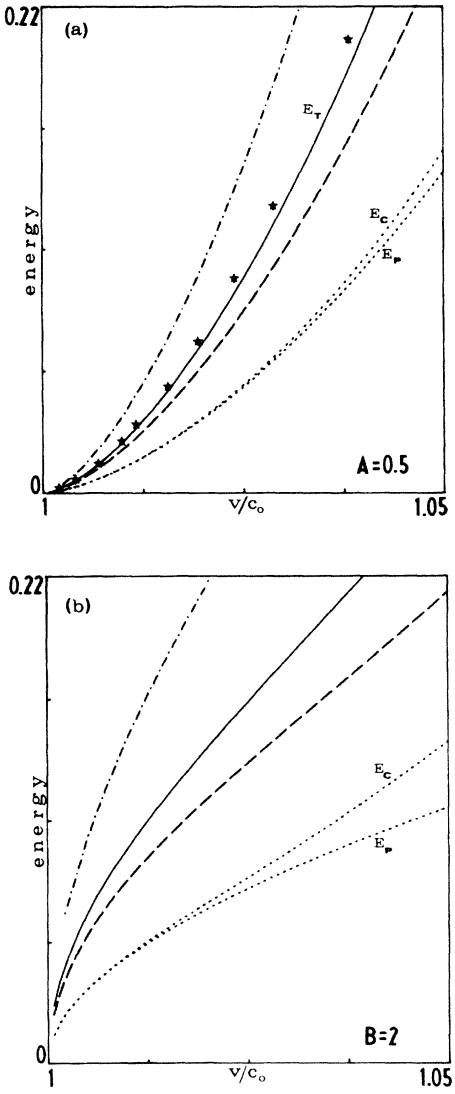

FIG. 3. Plot of the total energy E_t for a kink versus normalized soliton velocity v/c_0 for (a) a cubic and (b) a quartic interaction potential, for different mass ratios and without SNI, dashed, solid and dotted-dashed lines correspond to mass ratio $M_2/M_1=1$, 2, and 10, respectively, from the continuum-approximation results. Dotted lines indicate the potential (E_p) and kinetic (E_c) parts of the soliton energy for the case $M_2/M_1=2$, while stars correspond to simulation results for the same mass ratio.

a breather solution[28] that consists of a slowly varying amplitude of $O(1)$ and an oscillation with a long wavelength. The displacement of the odd atoms is given by

$$z(x,t)=\pm A_m \tan^{-1}\left[\frac{\beta}{\alpha}\operatorname{sech}\left[\frac{x-v_e t}{L_e}+x_1\right]\times\sin\left[\frac{x-v_0 t}{L_0}+x_0\right]\right], \quad (3.13)$$

with

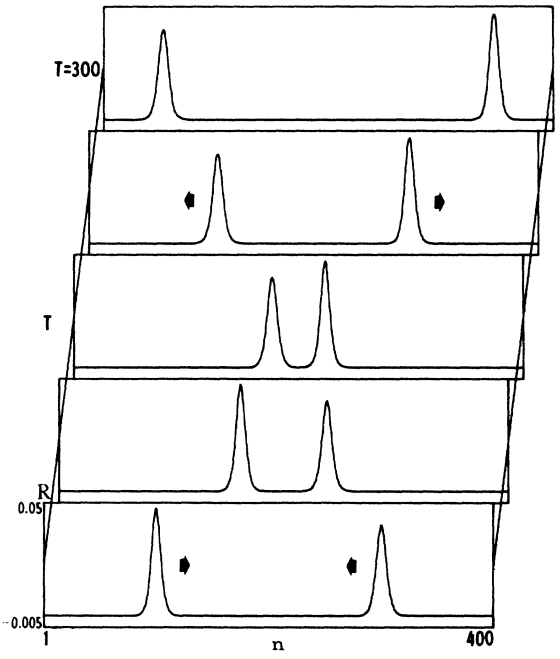

FIG. 4. Evolution and collision of two solitons in a diatomic chain with a cubic potential. Plot of the relative displacement. The initial conditions are two Bq solitons.

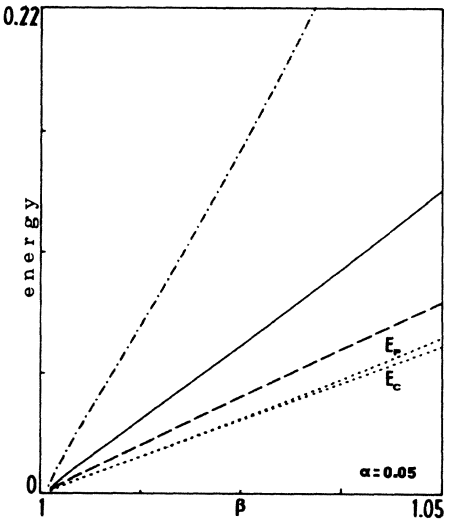

FIG. 5. Plot of the total energy for a breather versus the parameter β for various mass ratios $M_2/M_1=1$ (dashed line), 2 (solid line), 10 (dashed-dotted line). Dotted lines indicate the potential (E_p) and the kinetic energy (E_c) for the case $M_2/M_1=2$.

$$A_m=2\left[\frac{6h_0}{q_0}\right]^{1/2}, \tag{3.14}$$

$$v_e=c_0-2\frac{h_0}{c_0}(3\alpha^2-\beta^2),\quad L_e=\frac{1}{2\beta}, \tag{3.15a}$$

$$v_0=c_0-2\frac{h_0}{c_0}(\alpha^2-3\beta^2),\quad L_0=\frac{1}{2\alpha}, \tag{3.15b}$$

where α and β are small arbitrary parameters so that L_e and L_0 are large. The constants x_1 and x_0 indicate the initial position of the envelope and the oscillating wave form, respectively, while v_e and v_0 are their velocities which are close to the speed of sound. The M-KdV equation has a breather solution if h_0 and q_0 have the same sign ($p_0=0$). When both h_0 and q_0 change sign due to SNI, v_e becomes subsonic from supersonic or vice versa.

In Fig. 5 we plot the energy of a breather in a quartic potential without SNI as a function of the parameter β for different mass ratios. The energy is larger for M_1/M_2 departing from unity. If we include SNI, the energy can significantly increase if the SNI are additive or significantly decrease if they are competitive. Increasing the parameter β corresponds to increasing the velocity of the breather, and decreasing the width. The calculations are performed for a constant $\alpha=0.05$. It seems that in comparison with the kink solitons there are two arbitrary parameters (α and β). The extra restriction that v is very close to c_0 imposes a constraint on the possible values of α and β. Notice that in Fig. 5 the plot is linear as a function of β. When viewed as a function of v_e, the curve would have the same form as for the kink in a quartic potential (see Fig. 3) since β is proportional to $(v_e-c_0)^{1/2}$ if $\alpha=0$. For competitive interactions, however, the curve can depart from linearity much sooner. The breather soliton given by (3.13) is stable under collision,[24] it does not present a net compression or dilatation and the mass in excess to (M_1+M_2) for each cell vanishes to $O(\epsilon)$.

E. Optical mode ($\sigma=-M_1/M_2$) in the long-wavelength approximation

In this case the ansatz of (3.2) satisfies the compatibility conditions to $O(\epsilon^3)$. This is because the highest term is of $O(\epsilon^3)$ as is the case for the acoustic mode. We can then neglect higher than second derivatives and nonlinear terms that include derivatives. These order-of-magnitude arguments also determine the order of coupling between acoustic and optical modes.

From the compatibility conditions using $\sigma=-M_1/M_2$ we obtain the coefficients in (3.2) and

$$b_1=1, \tag{3.16a}$$

$$b_2=2\mu_0\left[\frac{1}{M_1}+2g_0\right], \tag{3.16b}$$

with the other coefficients b_3, b_4, and b_0 set equal to zero. The parameters μ_0 and g_0 are given in (3.4) and (3.5).

In this section we limit ourselves to a quartic interaction potential ($A=A_1=A_2=0$) with FNI and SNI while the more general potential will be discussed in Sec. IV. If the coefficients b_1 and b_2 are chosen as in (3.16), we obtain a single equation to be solved for the displacement of the odd atoms while that of the even atoms is given by (3.2) keeping only the first three terms [i.e., $O(\epsilon^3)$], with b_1 and b_2 given by (3.16). The equation for $z(x,t)$ is

$$z_{tt}+C_1z_{xx}+C_2z+C_3z^3=0\ , \tag{3.17}$$

with

$$C_1=\frac{2GD^2}{M_1+M_2}\left[1-2\left[g_1\frac{M_2}{M_1}+g_2\frac{M_1}{M_2}\right]\right]\ , \tag{3.18a}$$

$$C_2=\frac{2G}{\mu_0}\ , \tag{3.18b}$$

$$C_3=\frac{2B}{\mu_0}\left[\frac{M_1}{\mu_0}\right]^2\ . \tag{3.18c}$$

For $C_2>0$ ($G>0$), (3.17) has no stable large-amplitude solutions of $O(1)$ because the bonds are stretched beyond the inflection point of the interaction potential. If $C_2<0$ there are kink solutions[29] for z, giving us an optical kink for the diatomic chain,[15] which is unstable for FNI only.[24] This case is discussed elsewhere.[30]

For $C_2>0$ we can find oscillating solutions by transforming (3.17) into a nonlinear Schrödinger (NLS) equation for the slowly varying complex envelope function $F(x,t)$ if we look for solutions of the form

$$z(x,t)=F(x,t)e^{i(kx-\omega t)}+\text{c.c.}\ , \tag{3.19}$$

where k and ω are chosen to satisfy the linear dispersion relation $\omega^2=\omega^2(k)=C_2^2-C_1k^2$ at the center of the folded Brillouin zone ($k\simeq 0$) for the optical branch. By going into a reference frame moving with the group velocity $v_g=d\omega/dk=C_1k/\omega$, we obtain from (3.17) and (3.19) a NLS equation for the first harmonic $F(\xi,\tau)$, with $\xi=x-v_gt$ and $\tau=t$:

$$iF_\tau+\tfrac{1}{2}\mu F_{\xi\xi}+Q_0\,|F|^2F=0\ , \tag{3.20}$$

where we neglected terms like $F_{\tau\tau}$, and $\mu=d^2\omega/dk^2$ is related to the dispersion while

$$Q_0=-\frac{3C_3}{2\omega}\ . \tag{3.21}$$

The NLS equation for $\mu Q_0>0$ admits envelope solutions, which, for the discrete diatomic chain, define spatially localized envelope solitons in the form of a wave packet with an envelope function that modulates an essentially harmonic carrier wave.[18] For $\mu Q_0<0$ we have dark solitons,[21,24,31,32] where the envelope has a finite amplitude as $|\xi|\to\infty$ and a compression near the soliton position. Since $v_g\simeq 0$ near $k\simeq 0$, the sign of μQ_0 depends only on the parameter of the potential. Therefore, if $C_1C_3>0$, we have envelope solitons and if $C_1C_3<0$, we have dark solitons.

The envelope-soliton solution for $\mu Q_0>0$ with SNI is given by

$$z(x,t)=A_m\,\text{sech}\left[\frac{x-v_et}{L_e}+x_e\right]\cos\left[\frac{x-v_0t}{L_0}+x_0\right]\ , \tag{3.22}$$

with

$$\begin{aligned}&A_m=4\eta/(K_0)^{1/2},\quad K_0=Q_0/\mu\ ,\\ &v_e=v_g+2\alpha\mu,\quad L_e=\frac{1}{2\eta}\ ,\\ &v_0=[\omega+2\alpha v_g+2(\alpha^2-\eta^2)\mu]/(k+2\alpha)\ ,\\ &L_0=1/(k+2\alpha)\ ,\end{aligned} \tag{3.23}$$

where x_e and x_0 ($x_e=x_0$ in the simulations) indicate the initial position of the envelope and the carrier, while k, η, and α are small arbitrary parameters. Actually k and α come in the combination $k+2\alpha$ and the quantity in square brackets for v_0 is essentially $\omega(k+2\alpha)$ expanded in a Taylor series with a frequency shift of $-2\eta^2\mu$ due to nonlinearity. The actual wave vector and frequency of the carrier are small corrections from k and ω. The restrictions due to the scaling used in the approximations are that $A_m\sim\epsilon$, $k<0.1(\sim\epsilon)$, $v_e\ll 1$, $L_e\sim 1/\epsilon$, with ϵ the small scaling parameter.

IV. OSCILLATING SOLUTIONS WITH ARBITRARY WAVELENGTH

For envelope solitons with fast oscillations, we cannot expand the displacements z_{n+1} in Taylor series around z_n, and we must keep differences when fast changes are involved in the "carrier," while in the continuum limit treat the envelope part of the displacement that varies slowly (semidiscrete approximation). So we have automatically introduced two different space and time scales and the analysis can be done using the multiple-scales technique of reductive perturbation.[33] In this method the variables x or t are extended to many independent variables each with a different scale, i.e.,

$$x_n=\epsilon^nx,\quad t_n=\epsilon^nt,\quad n=0,1,2,\ldots\ . \tag{4.1}$$

A space or time derivative should be replaced by

$$\frac{d}{dx}=\sum_{n=0}^{\infty}\epsilon^n\frac{\partial}{\partial x_n},\quad \frac{d}{dt}=\sum_{n=0}^{\infty}\epsilon^n\frac{\partial}{\partial t_n}\ . \tag{4.2}$$

Because of (4.2) the method is also called the derivative-expansion method. In our case the variables $x_0=2nD$ (discrete) and $t_0=t$ in (4.1) come only in the phase $\theta=k\,2nD-\omega t$ and the derivative $\partial/\partial x_0$ in (4.2) is a difference operation for the discrete variable n. A general oscillating solution for the displacement of the odd atoms can be written in the form of an asymptotic series

$$\begin{aligned}z_n(t)&=\sum_l\epsilon^l\psi_l(n,t)\\ &=\sum_l\epsilon^l\sum_m F_{lm}(n,t)e^{im\theta(n,t)}+\text{c.c.}\ .\end{aligned} \tag{4.3}$$

The method is to substitute (4.1), (4.2), and (4.3) in (2.2) and equate powers of ϵ for the same harmonic. In general, the functions F_{lm} are coupled, but a few of them are needed to determine the solution to $O(\epsilon)$. In fact for a quartic potential only the term F_{lm} is needed and is decoupled from the others which contribute to $O(\epsilon^2)$. In what follows, we shall illustrate this case but we shall also present some numerical results for the cubic potential where more than one component is coupled, and the

analysis is quite more complicated since a different ansatz of (2.2) must be used for each F_{lm}.

For the quartic potential in the equation of motion (2.2) we substitute

$$z_n(t)=F_n(t)e^{i(2knD-\omega t)}+\text{c.c.}\ , \tag{4.4a}$$

$$w_n(t)=Q_n(t)e^{i(2knD-\omega t)}+\text{c.c.}\ , \tag{4.4b}$$

for the displacement of the odd and even atoms, respectively. In the resulting equations there are terms like $F_{n\pm1}$ or $Q_{n\pm1}$ which are expanded in a continuum approximation around $F(x,t)$ or $Q(x,t)$ with $2nD\to x$. Therefore, the fast changes of the phase $\theta=2knD-\omega t$ in (4.4) are correctly taken into account by taking differences in the phase for the discrete variable n. We obtain two equations for $F(x,t)$ and $Q(x,t)$, which can be decoupled using an ansatz similar to (3.2), i.e.,

$$Q(x,t)=\sigma e^{ikD}\left[F+b_1DF_x+\frac{b_2}{2}D^2F_{xx}+b_3DF_{xt}+b_0|F|^2F\right] . \tag{4.5}$$

In (4.5) the coefficients b_1, b_2, and b_3 are complex while b_0 and σ are real. To make the two equations for $F(x,t)$ identical we must also include (in comparison to the previous results) the terms F_{xt} and $|F|^2F$. The compatibility condition for the term proportional to F will give us the parameter σ which is equal to

$$\sigma=\frac{-\beta\pm\sqrt{\Delta}}{2\cos(kD)} , \tag{4.6}$$

with

$$\beta=-\left[1-\frac{M_1}{M_2}\right]-\left[g_1-\frac{M_1}{M_2}g_2\right][1-\cos(2kD)] , \tag{4.7a}$$

$$\Delta=\beta^2+4\frac{M_1}{M_2}\cos^2(kD) . \tag{4.7b}$$

The vanishing of the coefficient of F determines the dispersion relation to $O(\epsilon)$, i.e.,

$$\omega^2=\frac{2G}{M_1}[(1+g_1)-\sigma\cos(kD)-g_1\cos(2kD)]$$

$$=\frac{2G}{M_2}[\sigma(1+g_2)-\cos(kD)-\sigma g_2\cos(2kD)] . \tag{4.8}$$

Expressions (4.6) and (4.8) are the same as for the harmonic lattice as is seen in Fig. 6. The $+(-)$ sign corresponds to the acoustic (optical) branch of the dispersion relation. In the limit $k\to0$ we have $\sigma=1$ or $-M_1/M_2$, which is consistent with the result for the purely acoustic or optical mode in Sec. III. The compatibility conditions for the terms with F_x, F_{xx}, F_{xt}, and $|F|^2F$ will determine the parameters b_1, b_2, b_3, and b_0 correspondingly and their analytic expressions are given in the appendix. The coefficients of the other terms like F_t or F_{tt} can be identical in both equations. Using the transformations $\xi=x-v_gt$ and $\tau=\mu t$ in one of the two equations we again obtain a NLS equation as in (3.26) with $v_g=\partial^2\omega/\partial k^2$ being the group velocity and $\mu=\partial^2\omega/\partial k^2$ the second derivative of the dispersion corresponding to $\omega(k)$ given by (4.8)

$$iF_\tau+\tfrac{1}{2}\mu F_{\xi\xi}+Q_0|F|^2F=0 . \tag{4.9}$$

The parameter Q_0 in (4.9) is now given by

$$Q_0=\frac{3B}{\omega M_1}\left[\sigma^3\cos(kD)-\sigma^2[2+\cos(2kD)]+3\sigma\cos(kD)-1-8\frac{B_1}{B}\sin^4(kD)\right]+\frac{G}{\omega M_1}\sigma b_0\cos kD . \tag{4.10}$$

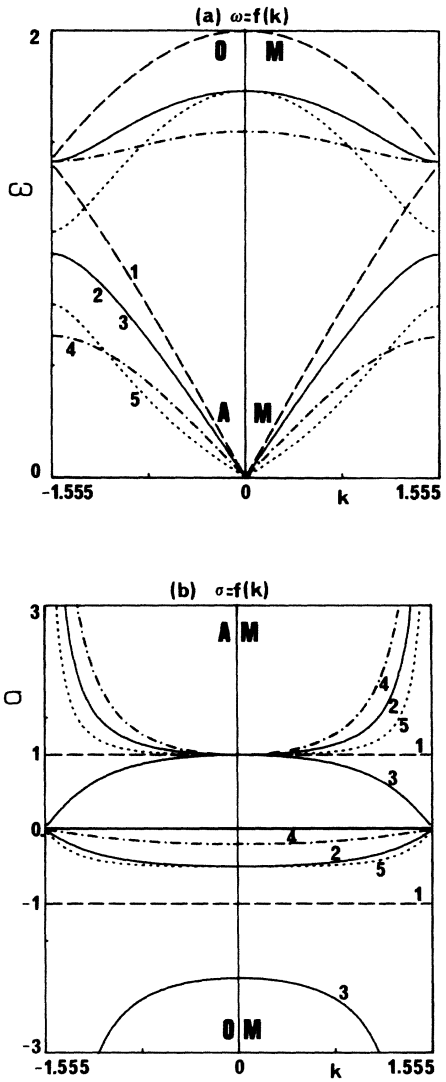

FIG. 6. Plot of (a) the dispersion relation $\omega(k)$ and (b) the parameter σ as a function of the wave vector k for different mass ratios, with $G=1$, $G_1=G_2=0$. 1 is monoatomic limit $M_1=M_2=1$ (dashed line). 2 is $M_2/M_1=2$ (solid line). 3 is $M_2/M_1=\frac{1}{2}$ (solid line). 4 is $M_2/M_1=5$ (dotted-dashed line). Positive values of σ define the acoustic branch (AM) and negative values define the optical branch (OM).

If $Q_0/\mu > 0$, Eq. (4.9) has envelope-soliton solutions with $z(x,t)$ given by relations similar to (3.22) and (3.23). The displacement of the even atoms is given by (4.4b) and (4.5) with the parameters b_1, b_2, b_3, and b_0 given in the appendix and σ from (4.6). In the limit $M_1 = M_2$ the above expressions reduce to those obtained for a monoatomic chain.[21,22] If $Q_0/\mu < 0$ in (4.9) we have dark solitons[24] which will not be discussed here.

The positive sign of Q_0/μ determines the existence of envelope solitons and the instability of plane waves due to modulation.[21,34] In Fig. 7, we plot the ratio $Q_0/\mu = K_0$ as a function of the wave vector k for the acoustic and optical branches of a diatomic chain with a quartic potential for three different cases for the SNI constants. For the acoustic branch without SNI or additive SNI there are envelope solitons, while for weakly competitive SNI near the center there are dark solitons. For the optical branch there is significant change only for strong additive SNI force constants [Fig. 7(b)]. The behavior near $\pi/2$ for both the optical and acoustic branches is dominated by the sign of the dispersion parameter μ. In fact, the existence of the gap in the dispersion relation for the diatomic chain as compared to the monoatomic chain strongly dominates the stability or not of plane waves near $\pi/2$.

In Fig. 8 we plot the energy of an envelope soliton as a function of the wave vector k for the acoustic and optical branches for different mass ratios. If there are no SNI the energy in the acoustic branch varies slowly except when we go to very different masses. In the optical branch, however, for $M_2/M_1 = 1$ the energy is almost a constant [dashed line in Fig. 8(b)], while for $M_2/M_1 = 2, 10$ it changes significantly with k due to the appearance of dark solitons at the k values where the energy of the envelope soliton vanishes. These conclusions for the energy and the amplitude of the envelope soliton can be generalized to SNI if we keep in mind the results of Fig. 7. This means that if the masses are not very different, the energy does not vary significantly with k except near the points where there is a change to dark soliton. The calculations have been done for constant values of α and η with $\alpha = 0.05$, $\eta = 0.1$, but small changes in α and η do not alter the results qualitatively except to raise or lower the curves for the energy.

The approximate solutions derived for the envelope solitons are also valid for the discrete lattice except for some small adjustment. In fact as we see in Fig. 9 (also see Fig. 10), the soliton does not change in form during propagation and the frequency of the carrier wave stays the same as observed in the time Fourier transform [Figs. 9(b) and 9(d)] of the atomic displacement of a particular light mass. In Fig. 9(a) we represent, in enlargement, the final

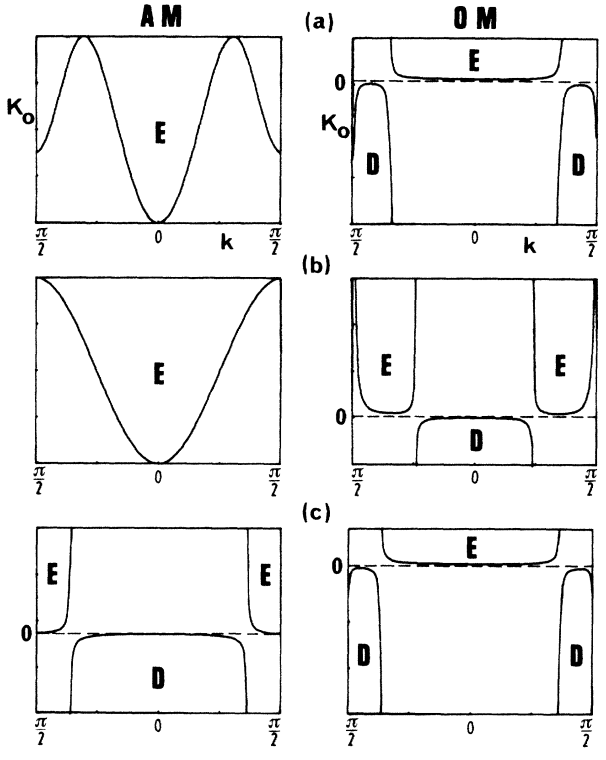

FIG. 7. Plot of the parameter $K_0 = Q_0/\mu$ versus the wave vector k for the acoustic (AM) and the optical (OM) branches of a diatomic chain with $M_2/M_1 = \frac{1}{2}$, $B = G = 1$, and $\alpha = 0.05$, $\eta = 0.1$. E denotes envelope solitons, D denotes dark solitons. (a) $G_1 = G_2 = 0$, (b) $G_1 = G_2 = 0.5$, (c) $G_1 = G_2 = -0.2$.

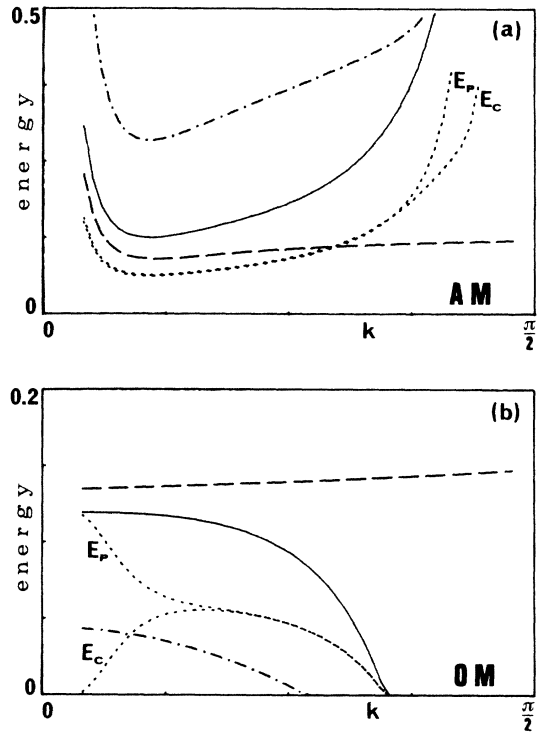

FIG. 8. Plot of the total energy for an envelope soliton versus the wave vector k for (a) the acoustic (AM) and (b) the optical model (OM), for different mass ratios and without SNI. Dashed, solid, and dotted-dashed lines correspond to mass ratios $M_2/M_1 = 1$, 2, and 10, respectively, from the continuum-approximation results. Dotted lines indicate the potential (E_p) and the kinetic (E_c) parts of the soliton energy for the case $M_2/M_1 = 2$.

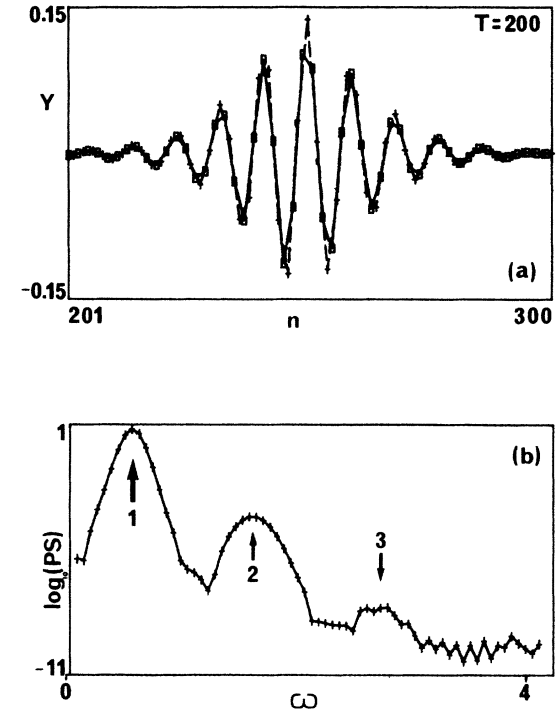

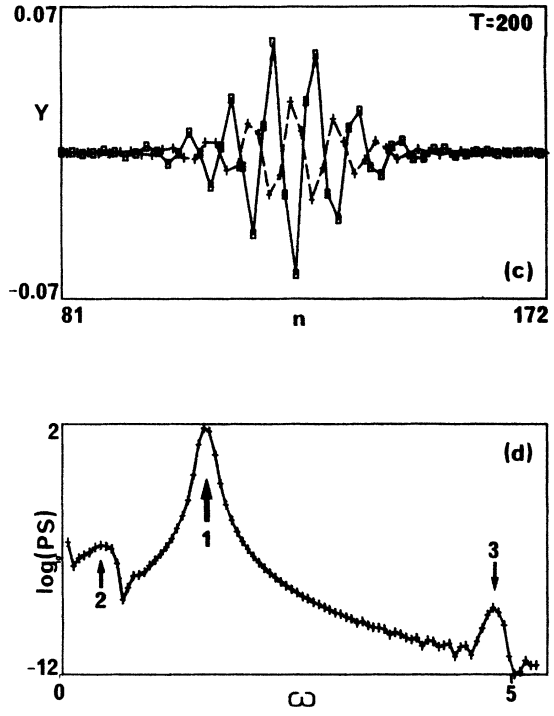

FIG. 9. Final state of a symmetric (a) acoustic ($k=0.8$, $\eta=\alpha=0.05$, $\sigma=1.15$) and (b) optical ($k=0.9$, $\eta=0.07$, $\alpha=0.05$, $\sigma=-0.41$) envelope solitons on a discrete diatomic chain ($M_2/M_1=2$) with a quartic interatomic potential ($G=B=1$) and without SNI. In (b) and (d) we represent the time Fourier transform of the motion of a light particle excited by the acoustic and the optical solitons, respectively.

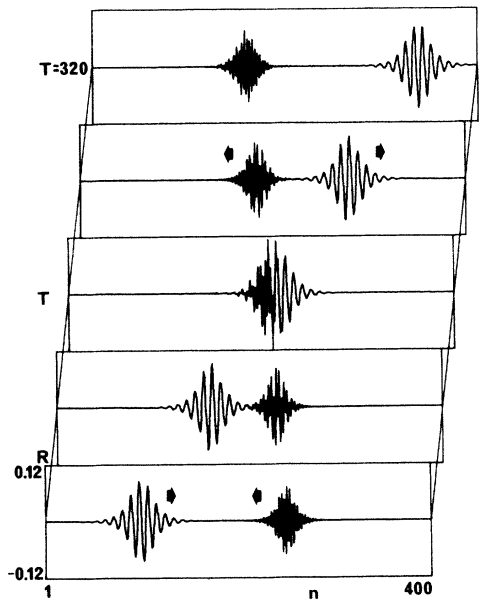

FIG. 10. Head-on collision between the two envelope solitons represented in Figs. 12(a) and 12(c).

state of an acoustic-envelope soliton after an evolution for 200 time units on a discrete diatomic chain ($M_2/M_1=2$), while in Fig. 9(c) we represent a similar plot for an optical-envelope soliton. In order to show the details of the acoustic and the optical character of the two solitons we denote separately the amplitude of displacements of the odd particles (squares connected by a solid line) and the amplitude of displacements of the even particles (crosses connected by a dashed line). For an initial condition with a carrier frequency $\omega=v_0/L_0=0.557$ in the acoustic branch, the time Fourier spectrum [Fig. 9(b)] is clearly dominated by one frequency $\omega_1=0.552$ indicated by arrow 1 in the figure. The second peak ($\omega_2=1.626$) is due to the coupling with the optical branch and the third peak ($\omega_3=2.638$) is the third harmonic. These last two peaks exist because these effects have been neglected in the analytical calculations as being small, which is consistent with the simulation results where the two extra peaks are 10^{-3} smaller in amplitude than the main peak. Similar conclusions are derived by the examination of the Fourier spectrum [Fig. 9(d)] for the optical soliton. As expected, the second peak which is due to the coupling between the two branches is observed in the acoustic region.

The stability of the envelope solitons is verified under collisions in a diatomic chain with quartic FNI, while the same is expected for a chain with cubic interatomic potential. In Fig. 10 we examine the head-on collision of the two previously studied envelope solitons. Here, we represent the evolution of the relative displacement for each particle of the diatomic lattice.

In Fig. 11 we studied the propagation of an envelope soliton in a chain with cubic plus quartic interatomic potential. In this case it can be shown there are asymmetric envelope solitons with different boundary conditions at $n\rightarrow\infty$ and $-\infty$ but we have not derived analytic expres-

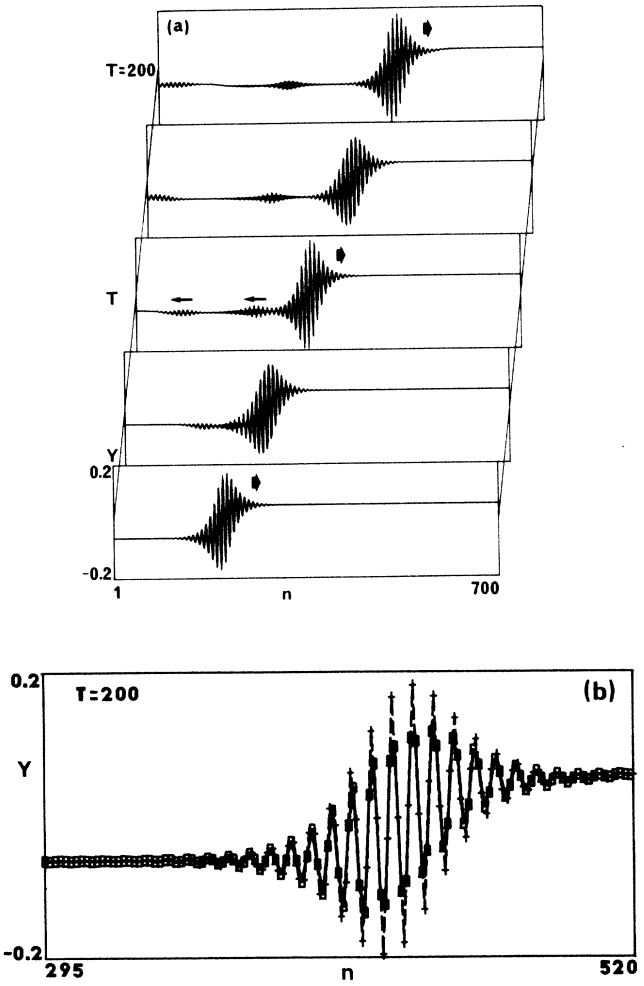

FIG. 11. Asymmetric envelope soliton with $k=0.9$, $\alpha=0.05$, and $\eta=0.03$ in a diatomic chain ($M_2/M_1=1.5$) with cubic and quartic FNI ($G=1$, $A=-0.5$, $B=1$) and harmonic SNI ($G_1=G_2=0.5$). The initial condition was that of a monoatomic chain. (a) evolution, (b) final state at time $T=200$.

sions since the calculation is very lengthy due to the coupling of many harmonics which, however, can be decoupled. The final result to $O(\epsilon)$ is the superposition of a kink of purely acoustic type and a symmetric envelope of the type calculated in this section with amplitudes which are related and moving as a coupled excitation. The initial condition of Fig. 11 is that for a monoatomic chain,[21] which soon adjusts itself to the lattice with $M_2/M_1=1.5$ and the excitation is stable. In Fig. 11(b), we show an enlargement of the details of the final soliton state after an evolution of 200 time units on the discrete diatomic lattice.

V. A MODEL OF TWO-PARALLEL CHAINS

The approximation of a single chain with longitudinal motion is an idealization that permits us to obtain exact solutions which can be used as prototypes. However, even in quasi-one-dimensional physical systems, we must consider the influence of the coupling to the surrounding chains. Such an extension together with the inclusion of transverse motion will lead us to the study of propagation of nonlinear excitations in three dimensions.[35] As a first step, the diatomic model presented here can be used directly to study the coupling of two monoatomic chains as in Fig. 12. It consists of two chains with different masses each coupled diagonally with two masses in the other chain. Now the FNI of the diatomic chain correspond to interchain interactions, while the SNI become interactions between nearest neighbors for each chain. In the new model both the interchain and the intrachain couplings can be nonlinear. If we assume that there is no transverse motion, then the solutions presented earlier can be directly applied so that z and w are the longitudinal displacements of the atoms in each chain.

While there is a strong similarity between the models of Fig. 1 and Fig. 12, the dynamical behavior can be quite different since the second case can correspond to a diatomic chain with weak FNI and strongly anharmonic SNI. This can make a difference on whether the kinks are subsonic or supersonic while the region of stability of plane waves could be very different. At the same time the coupling between the chains can induce collective motion on the other chain when one is excited. If the two chains are excited with initial displacements those of the diatomic chain the soliton can propagate even for the range of parameters of interest.[24] If, however, we excite a single chain, the response of the system is different when the initial excitation has a finite or zero mass. The reason is obvious since for finite mass the first chain has a net strain so that even for weak interchain coupling there is a large amount of energy. As a result, a kink is also created in the other chain with large-amplitude long-wavelength oscillations. On the contrary, if we excite on one chain an envelope soliton (zero mass), the second chain gradually (for weak coupling G) builds up the corresponding envelope soliton (see Fig. 13) and they propagate together. If the coupling is strong the violent transient behavior will not permit the creation of a coherent excitation. A particular case of this model is when one of the masses is much larger say $M_1 \gg M_2$. In particular, if $M_2 \sim O(1)$ and $M_1 \sim O(\epsilon^{-1})$ then this is a solution such that the leading term in z_n is of $O(\epsilon^2)$, while for w_n is of $O(\epsilon)$. For the appropriate choice of the signs of the force constants, with a cubic term in the interaction potential between chains, the solution is a kink of $O(\epsilon^2)$ along the chain of heavy atoms coupled to an asymmetric envelope for the light atoms. The asymmetric envelope consists of a sym-

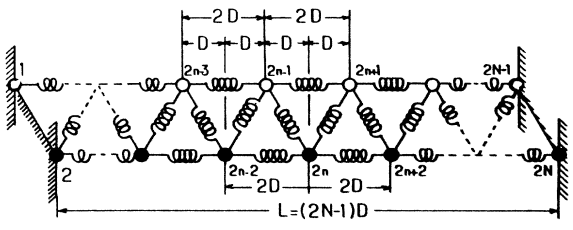

FIG. 12. The model of two parallel interacting chains.

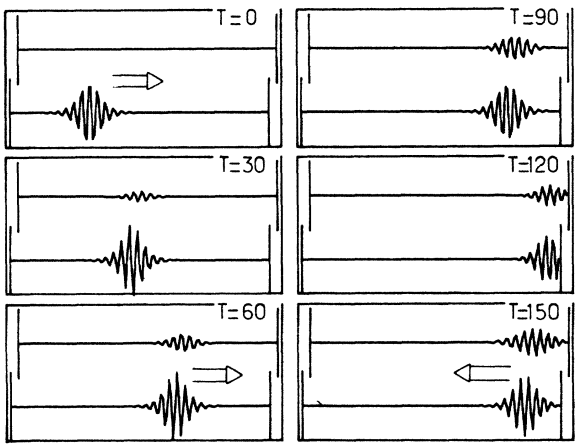

FIG. 13. The chain 1 (lower part of each figure) is excited by an envelope soliton, which is an exact solution of the uncoupled system. The coupling between the two chains ($G=0.01$, $A=B=0$) very quickly induces soliton motion on the other chain (upper part of each figure): $G_1=G_2=B_1=B_2=1$, $A_1=A_2=0$, $\eta=0.06$, $\alpha=0.01$, $k=0.82$.

metric envelope of $O(\epsilon)$ superimposed on a kink of $O(\epsilon^2)$. This problem is analogous to one in a different physical situation including electronic excitations considered by Davydov[36,37] in alpha helical proteins. This case will be studied in more detail later.

VI. SUMMARY AND CONCLUSIONS

In this paper we have studied the dynamics of acoustic and optical solitons in a nonlinear one-dimensional diatomic lattice model, in which the atoms interact with their first and second nearest neighbors following a nonlinear interatomic potential with harmonic, cubic, and/or quartic terms, which is simple enough so that analytic solutions can be obtained. The results, however, are expected to be valid for more realistic potential interactions (Buckingham, Lennard-Jones, Morse, etc.).[24]

We first used the continuum-limit approximation and demonstrated that the chain dynamics can be approximately described by nonlinear partial differential equations of the integrable or quasi-integrable type. This allowed us to calculate, within the long-wavelength limit, acoustic and optical solutions of the nontopological soliton type. We then used an analytical technique (semidiscrete approximation) which enabled us to calculate oscillating soliton solutions, of the pulse or kink type, modulating a quasiharmonic carrier wave, the wave vector of which is not limited by the continuum-limit approximation.

Table II summarizes soliton solutions for the nonlinear diatomic chain. Supersonic or subsonic kink excitations given by (3.10) with velocities close to the speed of sound c_0 propagate without modification in the discrete lattice. If the velocity deviates significantly from c_0, the kinks adjust by emitting the excess energy and modifying the soliton parameters as shown in Fig. 2. The oscillating solitons (envelope or dark), which propagate in a lattice with asymmetric potential (cubic or cubic + quartic), are likewise asymmetric (see Fig. 11). The solution is the sum of a kink and a symmetric envelope or dark soliton propagated at the same 'group' velocity. When the asymmetric (cubic) part of the potential vanishes the kink disappears and the oscillating soliton becomes symmetric (see Figs. 9 and 10).

The stability of oscillating solitons, and, therefore, the instability of plane waves, depend strongly on the potential parameters and the mass ratio M_2/M_1. In particular, the opening of a gap in the linear dispersion relation for the carrier wave [Fig. 9(a)] drastically alters the character of the solutions near $k=\pi/2$ (see Fig. 10). We also calculated the energy of each excitation and we find that for the same energy the widths of the three types of excitation are comparable. However, only an order-of-magnitude comparison can be made. This is because extra parameters characterize some of the solutions. However, in each case there can be a limitation on the possible numerical values of these parameters from order-of-magnitude arguments.

It would be interesting to extend the kink solutions to large velocities $v/c_0>1.5$, where we cannot use the continuum approximation and at present we do not have any analytic expressions. However, by considering the dynamics of a few atoms near the core of the soliton we can obtain relations between the physical parameters that characterize the soliton, i.e., amplitude and velocity, which are very different from those calculated in the continuum limit. This analysis along with computer simulations is published elsewhere.[23] These quasisoliton solutions would be very useful to study stable shock-wave propagation in solids.

The diatomic chain with a cubic nonlinearity has also been treated by Yajima and Satsuma with a different method and using new coordinates which to $O(\epsilon)$ are the center of mass and relative coordinates for the two masses. Their results are in qualitative agreement with ours and their solution corresponds to a particular solution in our case which is the asymmetric envelope soliton.

TABLE II. Nontopological soliton excitations in nonlinear diatomic chains.

Mode	Excitations	Equation model
Acoustic	Kink (pulse) soliton	Bq, M-Bq, G-Bq (or KdV, M-KdV, G-KdV)
	Breather soliton	M-KdV
	Envelope or dark soliton	NLS
Optical	Envelope or dark soliton	NLS

However, the instability they predict for $\frac{1}{2} < M_2/M_1 < 2$ is valid only for the acoustic branch near $k \sim 0$, where we expect to have asymmetric dark solitons, while very close to $k \sim 0$ special care is required. In fact for a general k the stability of the envelope solitons is always determined from the sign of Q_0/μ.

Recently Collins,[36] using some clever techniques, has applied a "semicontinuum" approximation (SCA) for the acoustic nonlinear excitations in a diatomic chain. The method is best suited for the acoustic-type excitations even though in principle it can be extended for the oscillating- and optical-type excitations using techniques similar to the multiscaling method described here. The main advantage of the SCA is that a general interatomic potential (GIP) with FNI can be easily treated, but the problem is more complicated with SNI. The GIP case does not alter the conclusions for the optical mode in Sec. III E since the amplitude is of $O(\epsilon)$ and (3.17) is consistent to $O(\epsilon^3)$.

In the simple model of two parallel chains we have shown that envelope solitons are less sensitive than kinks to the coupling with neighboring chains. This means that they also should be important dynamic excitations in one-dimensional macromolecular systems. Extensions of the diatomic chain model to include coupling between chains could be useful to treat realistic macromolecular systems,[11,37,38] while the inclusions of electronic charge with a polarizable ion which creates local nonlinearities has been used in the study of ferroelectrics.[7,8] The above results could also be generalized for spin systems with easy-plane anisotropy when the spins can be treated classically.[39] To examine the relevance of the nonlinear excitations in thermal conductivity and other mechanical properties, one must also consider their stability in a chain with impurities and also the effect of external forces (constant or oscillating) that could balance the energy loss due to inhomogeneities and their pinning due to discretization effects.

The analytic expressions for soliton excitations will permit us in the future to evaluate correlation functions and study the thermodynamics of these systems. The inclusion of transverse oscillations and the coupling with other chains would make the techniques described here applicable to study the dynamics of three-dimensional systems. As a first step we could consider surfaces where we can approximate the crystal as a static substrate potential for the atoms in the surface layers. Recent works in this direction seem hopeful.[40,41]

ACKNOWLEDGMENTS

We thank Dr. M. Peyrard for useful discussions. Part of this work was done under the Greek-French scientific agreement.

APPENDIX

The complex coefficients b_1, b_2, b_3, and b_0 used in the ansatz (4.5) for the oscillating soliton solutions so that the two equations for z and w are compatible are given as

$$b_1 = 1 + i\,\mathrm{Im}(b_1)\ , \tag{A1}$$

with

$$\mathrm{Im}(b_1) = \frac{\tan(kD)}{R}\left[\left(\frac{M_1}{\sigma M_2} - \sigma\right) - 4\left(g_1 - \frac{M_1}{M_2}g_2\right)\cos(kD)\right] = -\frac{1}{\sigma D}\frac{\partial \sigma}{\partial k}\ , \tag{A2}$$

where

$$R = \frac{M_1}{\sigma M_2} + \sigma \tag{A3}$$

and $\sigma(k)$ is given by (4.6). The coefficients b_2 and b_3 are

$$b_2 = \mathrm{Re}b_2 + i\,\mathrm{Im}b_2\ , \tag{A4}$$

where

$$\mathrm{Re}b_2 = 2\left[\frac{M_1}{\sigma M_2}\cos(kD) + \sigma\,\mathrm{Im}(b_1)\sin kD - 2\left(g_1 - \frac{M_1}{M_2}g_2\right)\cos(2kD) - 2\frac{M_1}{M_2}g_2\,\mathrm{Im}(b_1)\sin(2kD)\right] \Big/ [R\cos(kD)]\ , \tag{A5a}$$

$$\mathrm{Im}b_2 = 2\left[\frac{M_1}{\sigma M_2}\sin(kD) + \sigma\,\mathrm{Im}(b_1)\cos(kD) + 2\frac{M_1}{M_2}g_2\sin(2kD)\right] \Big/ [R\cos(kD)]\ , \tag{A5b}$$

$$b_3 = \mathrm{Re}b_3 + i\,\mathrm{Im}b_3\ , \tag{A6}$$

with

$$\mathrm{Re}b_3 = -\mathrm{Im}(b_1)\omega M_1/[GR\cos(kD)]\ , \tag{A7a}$$

$$\mathrm{Im}b_3=\omega M_1/[GR\cos(kD)]\ . \tag{A7b}$$

The coefficient of the nonlinear term is real and given by

$$b_0=3B\left[1-2\frac{M_1}{M_2}+2\sigma^2-\frac{M_1}{M_2}\sigma^2+\left[\frac{M_1}{\sigma M_2}+3\frac{M_1}{M_2}\sigma-\sigma^3-3\sigma\right]\cos(kD)\right.$$
$$\left.+\left[\sigma^2-\frac{M_1}{M_2}\right]\cos(2kD)+8\left[\frac{B_1}{B}-\frac{M_1}{M_2}\frac{B_2}{B}\sigma^2\right]\sin^4(kD)\right]\Big/[R\cos(kD)]\ . \tag{A8}$$

In the limit $M_2=M_1$ from (4.6) and (4.7) we get $\sigma=\pm1$. If we choose $\sigma=1$ (acoustic branch) then the real parts of b_1 and b_2 are equal to unity while $\mathrm{Re}b_3=0$ since $\mathrm{Im}b_1=0$. On the other hand since $F_{xt}\simeq-v_gF_{xx}+O(\epsilon^4)$ then the imaginary part of $(b_2D^2/2-v_gb_3D)$ in (4.5) also vanishes. The coefficient b_0 is equal to zero so that (4.5) is again a Taylor expansion for the even atoms about the odd atoms when $M_1=M_2$.

---

*Present address: Research Center of Crete, P.O. Box 1527, 71110 Heraklio, Crete, Greece.

[1]E. Fermi, J. R. Pasta, and S. Ulam, Los Alamos Scientific Report No. 1940, 1955 (unpublished).
[2]N. J. Zabusky and M. D. Kruskal, Phys. Rev. Lett. **15**, 240 (1965).
[3]N. J. Zabusky, Comput. Phys. Commun. **5**, 1 (1973).
[4]M. A. Collins, Adv. Chem. Phys. **53**, 225 (1983).
[5]M. Toda, J. Phys. Soc. Jpn. **22**, 431 (1967).
[6]F. Mokross and H. Büttner, J. Phys. C **16**, 4539 (1983).
[7]H. Bilz, H. Büttner, A. Bussmann-Holder, W. Kress, and U. Schörder, Phys. Rev. Lett. **48**, 264 (1982). See also Ferroelectrics **25**, 339 (1980).
[8]H. Büttner and H. Bilz, in *Recent Developments in Condensed Matter Physics,* edited by J. T. Devreese (Plenum, New York, 1981), Vol. 1.
[9]V. Ya. Antonchenko, A. S. Davydov, and A. V. Zolotariuk, Phys. Status Solidi B **115**, 631 (1983).
[10]M. J. Rice and E. J. Mele, Phys. Rev. Lett. **49**, 1455 (1982).
[11]A. Krumhansl and D. M. Alexander, in *Structure and Dynamics: Nucleic Acids and Proteins,* edited by E. Clementi and R. H. Sarma (Adenine, New York, 1983), p. 61.
[12]N. J. Zabusky and G. S. Deem, J. Comput. Phys. **2**, 126 (1967).
[13]J. Tasi and M. J. P. Musgrave, J. Mech. Phys. Solids **24**, 43 (1976).
[14]J. Tasi, Phys. Rev. B **14**, 2358 (1976).
[15]H. Büttner and H. Bilz, in *Solitons in Condensed Matter Physics,* edited by A. R. Bishop and T. Schneider (Springer, Berlin, 1978), p. 162.
[16]N. Yajima and J. Satsuma, Prog. Theor. Phys. **62**, 370 (1979).
[17]P. C. Dash and K. Patnaik, Prog. Theor. Phys. **65**, 1526 (1981).
[18]St. Pnevmatikos, M. Remoissenet, and N. Flytzanis, J. Phys. C **16**, L305 (1983). See also Helv. Phys. Acta **56**, 569 (1983).
[19]G. Behnke and H. Büttner, J. Phys. A **14**, L113 (1981).
[20]I. M. Torrens, *Interatomic Potentials* (Academic, New York, 1972).
[21]N. Flytzanis, St. Pnevmatikos, and M. Remoissenet, J. Phys. C **18**, 4603 (1985).
[22]St. Pnevmatikos, in *Singularities and Dynamical Systems,* edited by Sp. Pnevmatikos (North-Holland, Amsterdam, 1985). See also, C. R. Acad. Sci. Paris **296**, 1031 (1983).
[23]M. Peyrard, St. Pnevmatikos, and N. Flytzanis, Physica D (to be published).
[24]St. Pnevmatikos, Thèse d'Etat, Université de Dijon (1984). See also, Thèse de Troisième Cycle, Université de Dijon (1982).
[25]J. G. Berryman, Phys. Fluids **19**, 771 (1976).
[26]M. Wadati, J. Phys. Soc. Jpn. **38**, 673 (1976); **38**, 680 (1976).
[27]N. Flytzanis, St. Pnevmatikos, and M. Remoissenet, Physica D (to be published).
[28]G. L. Lamb, Jr., *Elements of Soliton Theory* (Wiley, New York, 1980).
[29]J. A. Krumhansl and J. R. Schrieffer, Phys. Rev. B **11**, 3535 (1975).
[30]St. Pnevmatikos, C. R. Acad. Sci. Paris **300**, 905 (1985).
[31]A. Hasegawa, *Plasma Instabilities and Nonlinear Effects* (Springer, Berlin, 1975).
[32]L. A. Ostrovsky, K. A. Gorshkov, and V. V. Papako, Phys. Scr. **20**, 357 (1979).
[33]T. Kawahara, J. Phys. Soc. Jpn. **35**, 1537 (1973).
[34]H. C. Yuen and W. E. Ferguson, Jr., Phys. Fluids **21**, 1276 (1978).
[35]J. H. Batteh and J. D. Powell, Phys. Rev. B **20**, 1390 (1979).
[36]M. A. Collins, Phys. Rev. A **31**, 1754 (1985).
[37]A. S. Davydov, Phys. Scr. **20**, 387 (1979); *Biology and Quantum Mechanics* (Pergamon, New York, 1982).
[38]A. C. Scott, Phys. Rev. A **26**, 578 (1982).
[39]H. J. Mikeska and E. Patzak, Z. Phys. **26**, 253 (1977).
[40]T. Sakuma and Y. Kawanami, Phys. Rev. B **29**, 869 (1984).
[41]E. W. Laedke and K. H. Spatschek, Phys. Rev. A **30**, 3279 (1984).